Horizontal displacements of reinforced soil walls from limit equilibrium calculations

Pietro Rimoldi
Consultant, Italy

ABSTRACT: The present paper is aimed to present a model for obtaining the horizontal displacements of reinforced soil walls directly from the results of LEM calculations in SLS conditions. Simplified yet realistic hypotheses are introduced on the distribution of the tensile force along each reinforcement layer; the isochronous curves of each type of reinforcement present in the wall design are used to evaluate the strains associated with the tensile force values, at different elapsed time from construction starting; the integral of the strains along each layer provides the horizontal displacement for that layer; corrections are introduced to reduce the displacements taking into account the stiffness of the facing system and the presence of total or partial restrain at toe. The proposed method has been validated with two instrumented walls, available in literature. It affords realistic value of horizontal displacements, yet still on the safe side, hence it can be a very valuable tool for performing the displacement analyses required in SLS conditions.

Keywords: displacements, wall, limit equilibrium, isochronous curves

1 INTRODUCTION

Limit Equilibrium Methods (LEM) are widely used for the design of reinforced soil walls (FHWA, 2009): these methods afford reliable values of the Factors of Safety (FS) for internal and external failure mechanisms, both in Ultimate Limit State (ULS) and Serviceability Limit State (SLS) conditions.

All LEM are based on equilibrium of forces and moments, hence they usually provide the maximum tensile force T_{max} along each reinforcement layer, required to satisfy all FS.

In SLS conditions required tensile forces are not critical, since they are always lower than in ULS conditions; but EuroCode 7 (EN 1997-1, 2004) and other norms require the evaluation of displacements and settlements in SLS conditions. The common practice is to use numerical models (either FEM or FDM) to perform calculations of displacements and settlements, but in this way all the advantage of LEM (simple and realistic models, easy to understand and correct) are lost.

For design purposes LEM are usually preferred to numerical models, while FEM or FDM are used for analyses, after the design has been done. But FEM / FDM models of such complicated structures, like e.g. a tiered reinforced soil walls with 4 different types of geogrids, are very time consuming, need a lot of input data which are not easily available, require validation by comparison with a known, monitored structure, and finally require a not easy critical judgement of results. In fact it is common experience with numerical models that a small variation just in one parameter brings to inconsistent results. Removing the inconsistencies of numerical models is always a difficult exercise.

On the other hand, LEM models, even for displacement calculations, are robust and easy to adjust, in case that some evident inconsistencies appear in results.

The present paper is aimed to present a new model for obtaining the horizontal displacements of reinforced soil walls directly from the results of LEM calculations in SLS conditions, which takes into account the position of the maximum tensile strength in each geogrid, the pullout anchorage length, the reduction of tensile strength at face, the total or partial restrain at toe, the face batter, the tiers and berms.

Simplified yet realistic hypotheses are introduced on the distribution of the tensile force along each reinforcement layer; the tensile curves and the isochronous curves of each type of reinforcement used in the wall design are used to evaluate the strains associated with the tensile force values, at different elapsed time from construction starting; the integral of the strains along each layer provides the horizontal displacement for that layer; corrections are introduced to reduce the displacements taking into account the stiffness of the facing system and the presence of total or partial restrain at toe.

The proposed method affords realistic value of horizontal displacements, yet still on the safe side, hence it can be a very valuable tool for performing the displacement analyses required in SLS conditions.

It is important to highlight that the tensile forces in the geogrids shall be calculated in serviceability conditions, that is by performing internal and external stability analyses with all amplifications and reduction factors set equal to 1.0.

2 DISPLACEMENT MODEL

Few preliminary considerations are required for the development of the wall displacement model:
- the proposed Displacement Model (DM) is applicable to reinforced soil wall, that is for retaining structures of either simple or complex geometry; the reinforcement types here considered are primarily geogrids, anyway it is applicable to other reinforcement types, like woven / knitted geotextiles, provided that the proper soil interaction factor for pullout is introduced;
- the DM is derived from LEM stability calculations, hence it is not aimed to follow the wall construction step by step, since this analysis can be performed only through sophisticated numerical models;
- hence the DM is aimed to just taking pictures of the wall face deformations at the end of construction (that is for elapsed time set equal to 1 - 3 months from placing the first geogrid layer), and at a later time, up to the end of the design life (set equal to 50 - 120 years).
- the DM affords to catch the results of all phenomena in a synthetic way; it is a Eulerian approach, not a Lagrangian approach, that means that we set the attention to what happens in a specific position (the face of the wall under examination) at a set point in time, rather than following each soil particle movement along elapsed time.
- all LEM models work following an Eulerian approach, and engineers usually like this approach since they prefer well defined pictures at different elapsed times, rather than blurred videos of the sequence of events.
- In this sense the Displacement Model works in this way:
  - forget what happens between zero time and 1 - 3 months (the construction time), and between 1 - 3 months and the selected post construction time (up to 50 - 120 years, end of design life);
  - concentrate on the instant picture of the wall at the end of construction and at the selected time;
  - evaluate the differences occurred in horizontal displacements between the end of construction and the selected time, that is the post construction displacements;
  - judge if the post construction displacements are acceptable and within the serviceability limit.

The DM has been developed based on the following assumptions (see the scheme in Fig. 1):
- Geogrids will not pull out of soil, since the wall is designed such that the anchorage length La is large and the Factor of Safety for pullot FS_{po} is always > 1.0 for each geogrid layer;
- Therefore each geogrid can elongate but it cannot pull out of the soil behind the potential failure line; hence strains in geogrids can occur only towards the wall face;
- Each geogrids will strain at any point at distance X_j from the face proportionally to the tensile force in that point $T(X_j)$, that is:

$$\varepsilon(X_j) = f(T(X_j)) \quad (1)$$

  where:
  $\varepsilon(X_j)$ = strain in the geogrids at distance X_j from the wall face.
- The function f(T(Xj) is derived from the isochronous curve of the geogrids at the selected time t;
- Two specific time instant are considered:
  - end of wall construction: considering the size and height of the walls, this time is set as 1 - 3 months from construction starting (that is from placing the first geogrid layer);
  - end of design life, set as 120 years from construction starting (that is from placing the first geogrid layer); different design lives can yet be considered, it is enough to use the related isochronous curves of the geogrid;

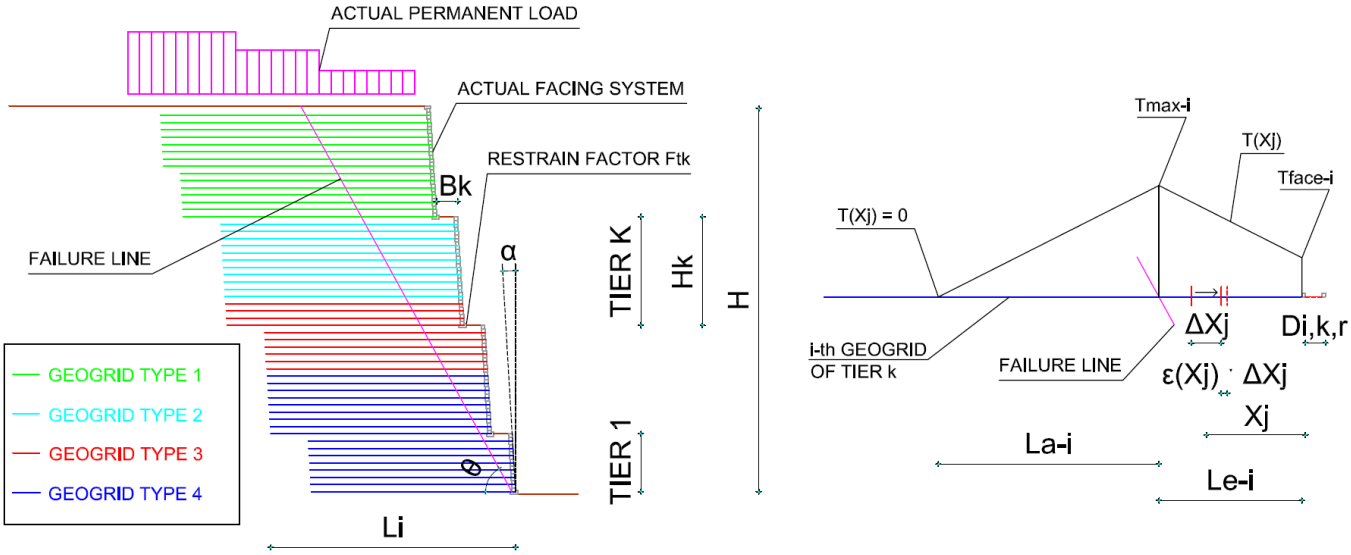

Figure 1. Scheme of the Displacement Model

- therefore the isochronous curves of the geogrids at 1 - 3 months and 120 years are used for the standard model;
- the isochronous curves are obtained from tensile creep test results at different temperatures, elaborated on the basis of the principle of time – temperature superposition, valid for polymeric products; these curves are usually expressed in the form T = f(ε); but for using Eq. (1) the isochronous curves need to be converted into the form ε = f(T). Usually these curves can be expressed, with very good approximation, by a third order polynomial function (for extruded geogrids) or by a fifth order polynomial function (for woven / knitted and bonded geogrids), hence in general:

$$\varepsilon = a\,T_{\%}^{5} + b\,T_{\%}^{4} + c\,T_{\%}^{3} + d\,T_{\%}^{2} + e\,T_{\%} \qquad (2)$$

where:
$T_{\%} = T / T_{ult}$
T = tensile strength under consideration (kN/m)
T_{ult} = ultimate tensile strength of the geogrids (kN/m)
a, b, c, d, e = parameters of the polynomial function;

- it is assumed that there is perfect congruency between the strains and displacements of the geogrids and of the soil interlocked in the geogrids:
- since the geogrid cannot strain towards the back, it can only strains forwards, towards the wall face;
- the displacement at point X_j is contrasted by all the soil between X_j and the face, which will compress and react as a spring with dashpot;
- along the potential failure line, in the point where the maximum tensile strength T_{max} occurs, at distance L_e from the face, the geogrid will elongate and the soil will move congruently with the geogrid; but the soil between the face and the potential failure line will resist the movement and will produce a counter thrust, which in turn will reduce the tensile force and the strain in the geogrid from the failure line towards the face;
- in the tie-back method used for designing reinforced soil walls with extensible reinforcement, the potential failure line is assumed to coincide with the Rankine failure line, that is a straight line with inclination θ equal to:

$$\theta = (45 + \varphi / 2) \qquad (3)$$

where:
θ = inclination of the potential failure line on horizontal (deg)
φ = friction angle of fill soil (deg)

Hence the distance L_{e-i} between the wall face and the failure line for the i-th geogrid at elevation h_i on the base (in case, part of tier k of the wall) considering the face batter α (constant for all tiers), is:

$$L_{e-i} = (h_i / \tan \theta) - (k - 1) \cdot B_k - h_i \tan \alpha \quad (4)$$

where:
h_i = elevation of i-th geogrids on the wall toe (m)
k = consecutive tier from bottom
B_k = width of berm on top of tier k (m)
α = batter of wall face from vertical (deg).

- The tensile force at face T_{face} will depend on the distance between the face and the potential failure line: in fact it is obvious that at wall bottom the face is very close to the potential failure line, hence T_{face} will be just slightly lower than T_{max}; while at the top of the wall there is a much larger distance between the face and the potential failure line, hence there will be a much higher decrease of T_{face} compared to T_{max}. Assuming that the variation of T between T_{max} and T_{face} is approximately linear, it is possible to evaluate T_{face-i} for the i-th geogrid layer, as:

$$T_{face-i} = T_{max-i} \cdot (H - h_i) / H \quad (5)$$

In favor of safety, the following limitation can be set:

$$T_{face} \geq 0.4\, T_{max} \quad (6)$$

where:
H = wall height (m)

- At the other side of the potential failure line the tensile strength of the geogrids will decrease according to the pull out resistance provided by the soil interlocked in the geogrids. The anchorage length L_a is the length beyond the failure line required to fully anchor the tensile strength T_{max}. At distance L_a from the failure line the tensile strength of the geogrids is assumed to become equal to zero. The anchorage length L_{a-i} for the i-th geogrid can be calculated with the pullout equation:

$$L_{a-i} = T_{max-i} / (2\, f_{po} \cdot \sigma_{vi} \cdot \tan \varphi) \quad (7)$$

where:
f_{po} = pullout factor
σ_{vi} = vertical stress on the i-th geogrid (kPa)
φ = friction angle of fill soil (deg)

- Considering that the displacements calculation is performed in serviceability conditions, the vertical stress σ_{vi} in Eq. (7) shall be calculated as the geostatic pressure due to the self weight of the soil above and the permanent surcharge, without any accidental surcharge.
- At distance L_{a-i} from the failure line the tensile strength of the geogrids is assumed to become equal to zero, hence:

$$T(X_j) = 0 \quad \text{for} \quad X_j \geq (L_{e-i} + L_{a-i}) \quad (8)$$

- Assuming that the variation of $T(X_j)$ between T_{max} and T_{face}, in the active wedge, and between T_{max} and zero beyond the failure line, is linear, the tensile strength in the i-th geogrid at any point X_j is:

$$T_i(X_j) = T_{face-i} + (T_{max-i} - T_{face-i}) \cdot X_j / L_{e-i} \quad \text{for } X_j \leq L_{e-i} \quad (9)$$

$$T_i(X_j) = T_{max-i} - T_{max-i} \cdot (X_j - L_{e-i}) / L_{a-i} \quad \text{for } X_j > L_{e-i} \quad (10)$$

- if the face cannot resist the movement of the soil, then each segment of geogrids will strain and the soil will move forwards without any contrast; therefore, in the situation where the wall has no facing or very flexible facing, the residual tensile strength of the geogrids at the face T_{face} will be equal to

zero (or according to Eq. 6), and the displacement D_{ik} of the wall face at the i-th geogrid level of tier k will be equal to the integral of the elongations of the i-th geogrid:

$$D_{ik} = \Sigma\, \varepsilon(X_j) \cdot \Delta X_j \qquad (11)$$

where:
X_j = distance of j-th point along the geogrid from the face (m)
ΔX_j = calculation segment over which ε can be considered as constant (m);

- if the wall face resists to horizontal displacements, then the residual tensile strength of the geogrids at the face T_{face} will be higher than zero, yet lower than T_{max}; such tensile strength T_{face} will stress the face elements; if these elements resist the stress (by friction, interlocking, mechanical connection, etc.) then they will produce a force that is equal and opposite to the tensile force T_{face}. The displacement of the face D_{ik} will still be given by Eq (11) but the distribution of $T(X_j)$ will be different than in the previous case.
- If there is a restrain at the toe of the wall and at the toe of each tier, like a foundation slab which limits or totally prevents the horizontal movement of the toe itself, the displacement D calculated with Eq. (11) has to be reduced accordingly; such reduction will be maximum at toe and lower and lower while the height over the toe or the berm increases. We can reasonably assume that the decrease in horizontal displacement is inversely proportional to the height over the toe or berm. Moreover we have to consider the consistency of restrain, through a Restrain Factor F_t, which will assume the value of 1.0 for perfect restrain, and a value of zero for no restrain. Hence for the i-th geogrid layer of tier k, considering perfect restrain at toe, the reduced horizontal displacement for the i-th geogrids becomes:

$$D_{i,k,r} = D_{i,k} \cdot (1 - (H_k - h_{i,k}) / H_k) \qquad (12)$$

where:
$D_{i,k,r}$ = reduced horizontal displacement of the i-th geogrid layer tier k due to restrain at toe (m)
$D_{i,k}$ = horizontal displacement of the i-th geogrid layer of tier k without restrain at toe (m)
H_k = height of tier k (m)
$h_{i,k}$ = height of the i-th geogrids on the toe of tier k (m)

- When specifically dealing with the general situation of tiered walls (where a simple wall can be considered just a tiered wall with 1 tier only), the following considerations are introduced:
  - If we take a picture of a tiered wall at 1 - 3 months or 120 years after construction has started, for sure the second tier, third tier, etc., will have travelled sitting on first tier, second tier, etc., hence the final position of the face has to take into account all the successive movements of what is below.
  - But the movement of the second tier as a consequence of the movement of the first tier is like shifting forward the seat of the car, yet the passenger of the second tier doesn't get an internal deformation of itself as a consequence of the seat movement.
  - If we stack some shoe boxes and we move slowly the bottom box, all other boxes will move as well, but these other boxes will not deform.
- About the movement of the tier on top as a consequence of the movement of the tier at bottom:
  - if we follow the construction steps, like we can do with a good FEM software, then when we load the second tier on the first tier, then the first tier will deform forwards and will carry forwards also the second tier, and so on;
  - but the present Displacement Model is derived from LEM calculations, hence displacements are calculated for each layer based on the tensile strength generated in geogrids when the wall is fully built;
  - therefore the successive displacements of each layer and hence of each tier are already synthetically included;
  - hence the displacements calculated by the DM are already the final ones after all construction steps and related movements have occurred.
- As example, let's consider a wall with height H = 23.32, made up of 4 tiers and 3 berms, each one 1.25 m wide (see the example at point 3). The second tier is 1.25 m back the top of the first tier; the moving portion of the first tier is the wedge limited by the failure surface and the anchorage (or

pullout) length; behind the pullout line there is no tension in geogrids, hence there is no displacement as well; at the top of the first tier the pullout line would pass approx at the toe of the second tier.
That is, the second tier is sitting on the stable portion of the first tier.
Therefore the displacement of the first tier has no effect on the displacements of the second tier.
The third and the fourth tiers would sit on a small portion of the moving part of the tier below, hence even here the displacement of the tier below has little effect on the movement of the tier above.
That's exactly why it is good to introduce berms and to design a tiered wall rather than a full height single tier one: the sum of displacements of each tier is lower than the displacement of the full height single tier.

- The displacement produced by the bottom tier on the top tier has the equivalent effect of a non perfect restrain at toe of the tier above. Hence this effect can be introduced in the DM in a simple and rational way by limiting the restrain at each tier toe, through the now introduced Restrain Factor at toe F_t; only if F_t is set equal to 1.0 the restrain is perfect and the toe of each tier will not move at all; while for $F_t < 1.0$ the toe is allowed to get a portion of the horizontal movement of the tier below.
- Hence with partial restrain at toe Eq. (11) becomes:

$$D_{i,k,\,r} = F_{tk} \cdot D_{i,k} \cdot (1 - (H_k - h_{i,k}) / H_k) \qquad (13)$$

where:
F_{tk} = Restrain Factor at toe of tier k.

Note:
F_{tk} = 1 for perfect restrain (no horizontal movement at toe);
F_{tk} = 0 for no restrain (free horizontal movement at toe).

- The serviceability limit shall refer to post construction displacements, which are equal to the difference between the displacements at 120 years (or at set post construction time) and the displacements at 1 - 3 months; such differential displacement is due to the tensile creep of the geogrids; hence for the serviceability limit we shall consider:

$$\Delta D_{i,r} = D_{i,k,\,r}\ (t = 120 \text{ years or set time}) - D_{i,k,\,r}\ (t = 1 - 3 \text{ months}) \qquad (14)$$

- An acceptable serviceability limit for the horizontal displacement of the face of a reinforced soil wall, which is a flexible structure, can be reasonably set as:

$$\Delta D_{i,r} \leq H / 200 \qquad (15)$$

If the differential displacement calculated with Eq. (14) respects the condition in Eq. (15), the serviceability limit on horizontal displacement shall be considered as verified.

- The post construction creep strain of the structure, that is of the whole reinforced block, can be calculated at each geogrid level, by dividing the total post construction displacement (from Eq. 14) by the geogrid length (equal to the width of the reinforced soil block):

$$\Delta\varepsilon_{ij\text{-structure}} = \Delta D_{i,r} / L_i \qquad (16)$$

where:
L_i = total length of the i-th geogrid (m).

- It is easy to understand that serviceability limits, like in Eq. (15), are applicable only to the wall structure, and not to each single geogrid reinforcement: hence setting limits to the post construction strain of each geogrid (e.g. post construction internal strains of the geogrid ≤ 0.50 %, like at point 6.5.5.2 and Tab. 19 of BS 8006: 2010) is totally meaningless.

3 EXAMPLE OF DISPLACEMENTS CALCULATION

The application of the Displacement Model is illustrated with reference to a complex wall, as shown in Fig. 2, with four tiers for a total height of 23.32 m, with relatively small hollow concrete block facing (0.40 m x 0.30 m x 0,22 m), reinforced with extruded geogrids of 60, 90, 140, 170 kN/m tensile strength,

which afford a pullout factor f_{po} = 1.00. The fill has a friction angle of 38° and a unit weight of 20.5 kN/m^3. The berms are all 1.25 m wide and the face batter of all tiers is 4°.

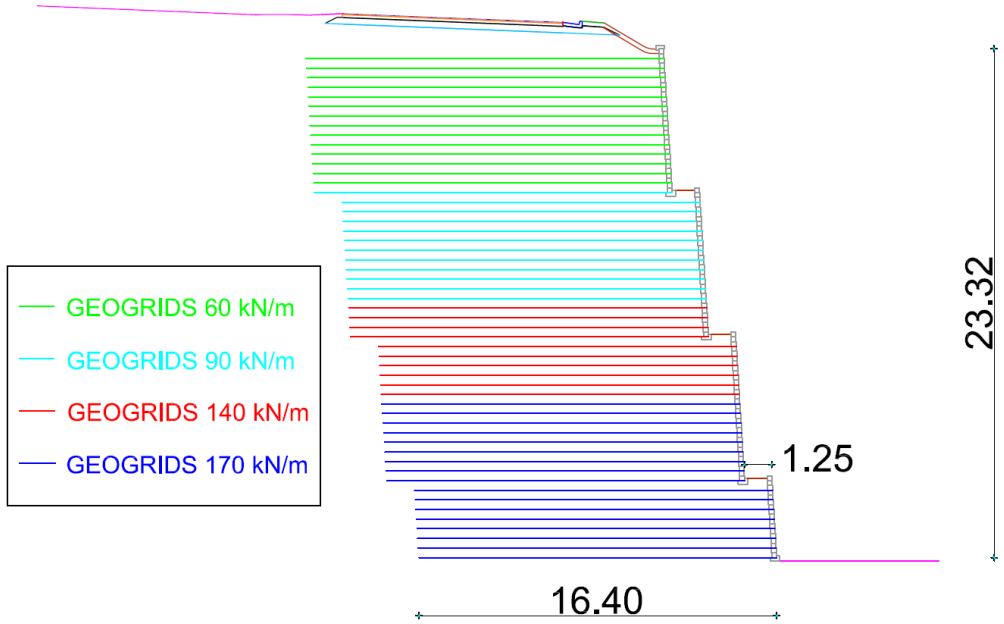

Figure 2. Reinforced soil wall for example

The maximum tensile force T_{max} in each geogrid has been calculated with MSEW (3.0) software (ADAMA, 2015), in serviceability conditions, that is with all amplifications and reduction factors set equal to 1.0. Results of the stability analysis in serviceability conditions, for the first two tiers, are reported in Tab. 1.

Table 1. Results of stability calculations for two tiers of the example wall

#	Geogrid Elevation [m]	Tavailable [kN/m]	Tmax [kN/m]	Tmd [kN/m]	Specified minimum Fs-overall static	Actual calculated Fs-overall static
1	0.00	66.9	26.5	N/A	1.000	2.526
2	0.44	66.9	52.2	N/A	1.000	1.280
3	0.88	66.9	51.3	N/A	1.000	1.304
4	1.32	66.9	50.3	N/A	1.000	1.328
5	1.76	66.9	49.4	N/A	1.000	1.353
6	2.20	66.9	48.5	N/A	1.000	1.380
7	2.64	66.9	47.5	N/A	1.000	1.407
8	3.08	66.9	46.6	N/A	1.000	1.435
9	3.52	66.9	45.7	N/A	1.000	1.465
10	3.96	66.9	44.7	N/A	1.000	1.495
11	4.40	66.9	43.8	N/A	1.000	1.527
12	4.84	66.9	42.8	N/A	1.000	1.561
13	5.28	66.9	41.9	N/A	1.000	1.596
14	5.72	66.9	41.0	N/A	1.000	1.632
15	6.16	66.9	40.0	N/A	1.000	1.670
16	6.60	66.9	39.1	N/A	1.000	1.710
17	7.04	66.9	38.2	N/A	1.000	1.752
18	7.48	49.2	37.2	N/A	1.000	1.320
19	7.92	49.2	36.3	N/A	1.000	1.354
20	8.36	49.2	35.4	N/A	1.000	1.390
21	8.80	49.2	34.4	N/A	1.000	1.427
22	9.24	49.2	33.5	N/A	1.000	1.467
23	9.68	49.2	32.6	N/A	1.000	1.509

The isochronous curves of the extruded geogrids, at 3 months and at 120 years, are shown in Fig. 3 left; from these curves the curves $\varepsilon = f(T / T_{ult})$ have been calculated and plotted in Fig. 3 right; the best interpolation is obtained with third order polynomials, whose parameters a, b, c are shown in Fig. 3 right.

Displacements calculation has been performed for all geogrid layers, according to the formulas of the Displacement Method.
For each geogrid the geogrid length $(Le + La)_i$, where strains occur, has been divided in 20 equal parts, each at distance X_j from the face.
The tensile strength $T(X_j)$, the strain $\varepsilon_{ij}(T)$ at 3 months and 120 years, and the local strain ε_{ij} $(T(X_j))$, at 3 months and 120 years has been calculated at each point X_j of the i-th geogrid, as shown in Fig. 4, referred to geogrid Nr 18, part of the second tier.

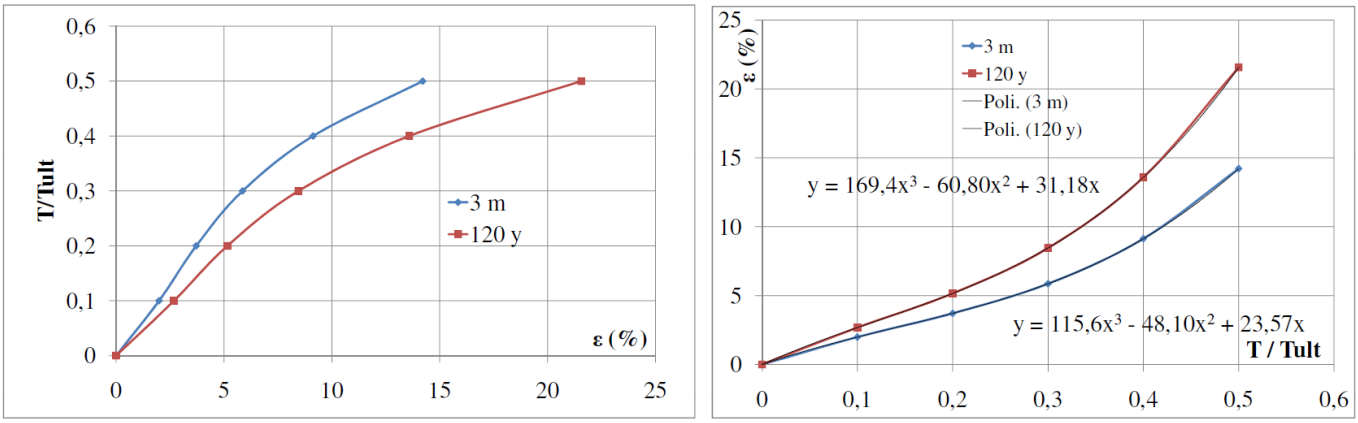

Figure 3. Isochronous curves at 3 months and 120 years (left) and curves $\varepsilon = f(T / T_{ult})$ with interpolation polynomials (right) for the extruded geogrids of the example wall

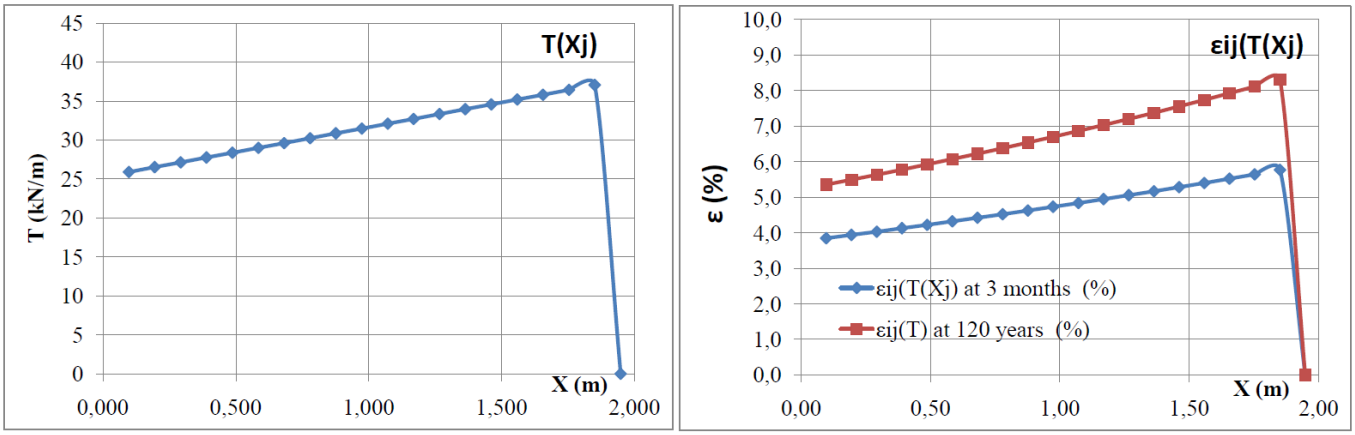

Figure 4. Tensile strength $T(X_j)$ and strain $\varepsilon_{ij}(T)$ at 3 months and 120 years, referred to geogrid Nr 18, part of the second tier of the example wall

Then the displacements of the face D_i of the wall with no facing, that is with $T(X = 0) = 0$, have been calculated at 3 months and 120 years.
By applying the restrain at toe with the Restrain Factor $F_t = 0.80$ (taking into account that each tier will "transport" forward the following tier), the reduced displacement of the face $D_{i,r}$ at 3 months and 120 years have been calculated.
The difference $\Delta D_{i,r}$ between $D_{i,r}$ at 120 years and at 3 months provides the post construction displacement.
Results, reported in Fig. 5, show that the maximum differential displacement between 3 months and 120 years is between 20 mm and 40 mm for each tier.
Such maximum post construction displacements also respect the serviceability limit in Eq. (15).
In Fig. 5 right it is evident that each subsequent tier is "transported" forward by the movements of the tiers below: this confirms that the use of the Restrain Factor is a very simple yet effective way to reproduce such effect in calculations.

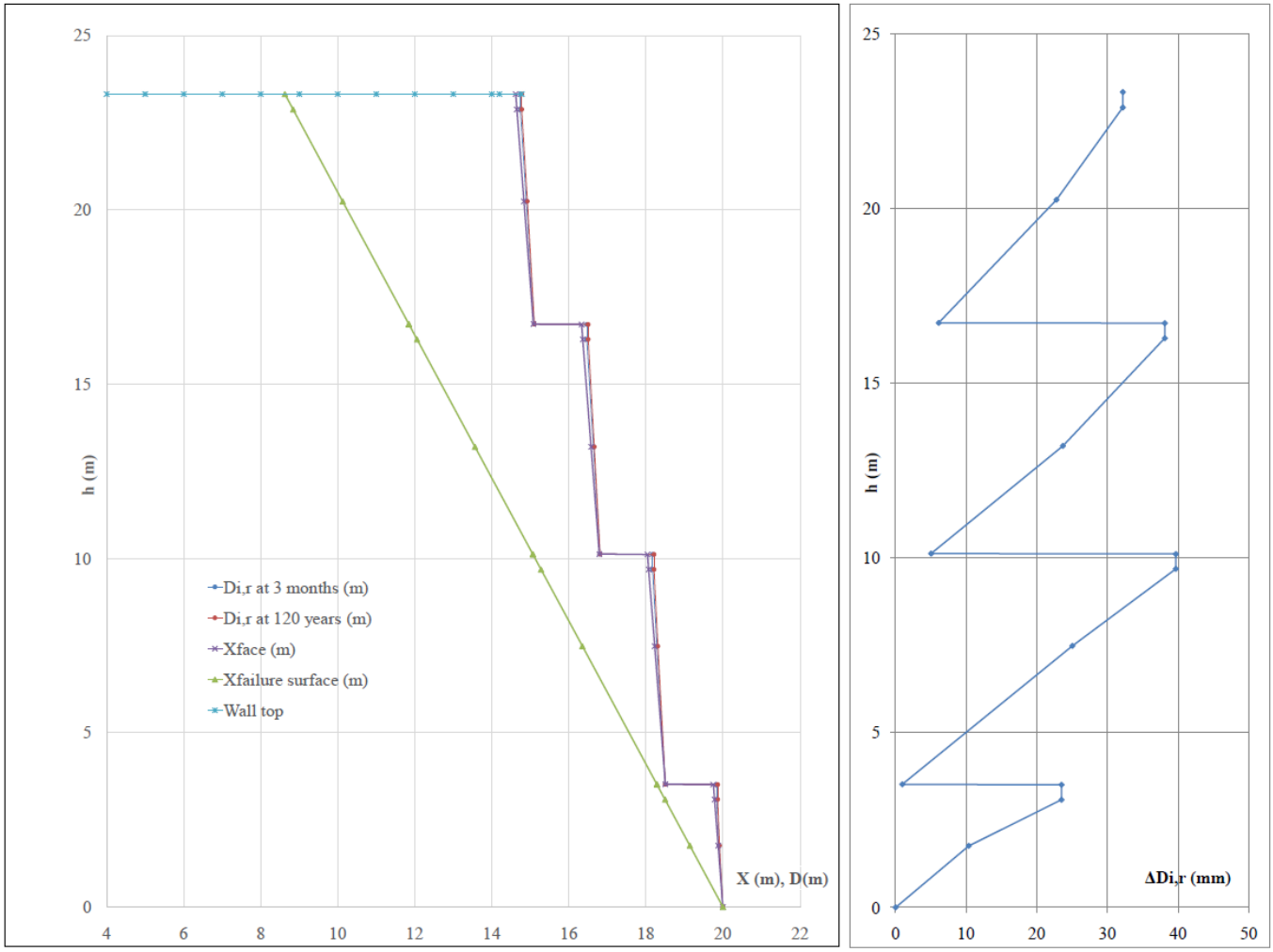

Figure 5. Results of displacement calculations for the example wall

4 VALIDATION OF THE DISPLACEMENTS MODEL

The Displacement Model has been validated by carrying out calculations for two walls for which measurements of horizontal displacements are available in literature:

1) The 8 m high wall built in Japan, described by Dobie and McCombie (2015) and Onodera et Al (2004), with relatively large concrete block facing, for which displacements measurements at end of construction and at 8 years post-construction are available;
2) the 16 m high wall, built in Izmir (Turkey), with massive gabion facing, for which displacements measurements at end of construction and FDM modeling are available (Gu et Al, 2017).

4.1 *Validation with Dobie and McCombie (2015)*

According to Dobie and McCombie (2015), a trial reinforced soil retaining wall was built in Japan in 1995, and has been reported by several authors in a number of papers. Some of the earliest information was provided by Nakajima et al (1996) and later by Tsukada et al (1998). The wall is 8 m high with a vertical precast concrete block facing, as shown in Fig. 6. The fill was reinforced with 11 layers of a relatively low strength HPDE reinforcement, manufactured by a process of punching and stretching (Tensar SR55 extruded uniaxial geogrids). All layers are 6 m long and have the same strength, with a layout as shown in Figure 6. A sand fill was used with unit weight γ = 18.6 kN/m^3; in the SLS calculation, φ_{peak} = 37° has been used. The trial wall was built at a testing facility and is not part of a permanent structure. A uniform surcharge of 9.8 kPa was placed on top of the fill, which is considered to be a dead load. More recent information was presented by Onodera et al (2004), providing lateral wall movement data after 8 years.

New analyses by Dobie and McCombie (2015) afforded the profile of the lateral movement at Day 11 (set as the starting point in time), and at Day 732 (about 2 years later): the wall has tilted forwards slightly, by about 30 mm at the top, but has remained essentially straight, and there is no noticeable sign of bulging. For validating the Displacement Method, for the cross-section in Fig. 6 stability analyses were back carried out with MSEW (3.0) software (ADAMA, 2015), affording the maximum tensile strength required for each geogrid layer, as reported in Tab. 2.

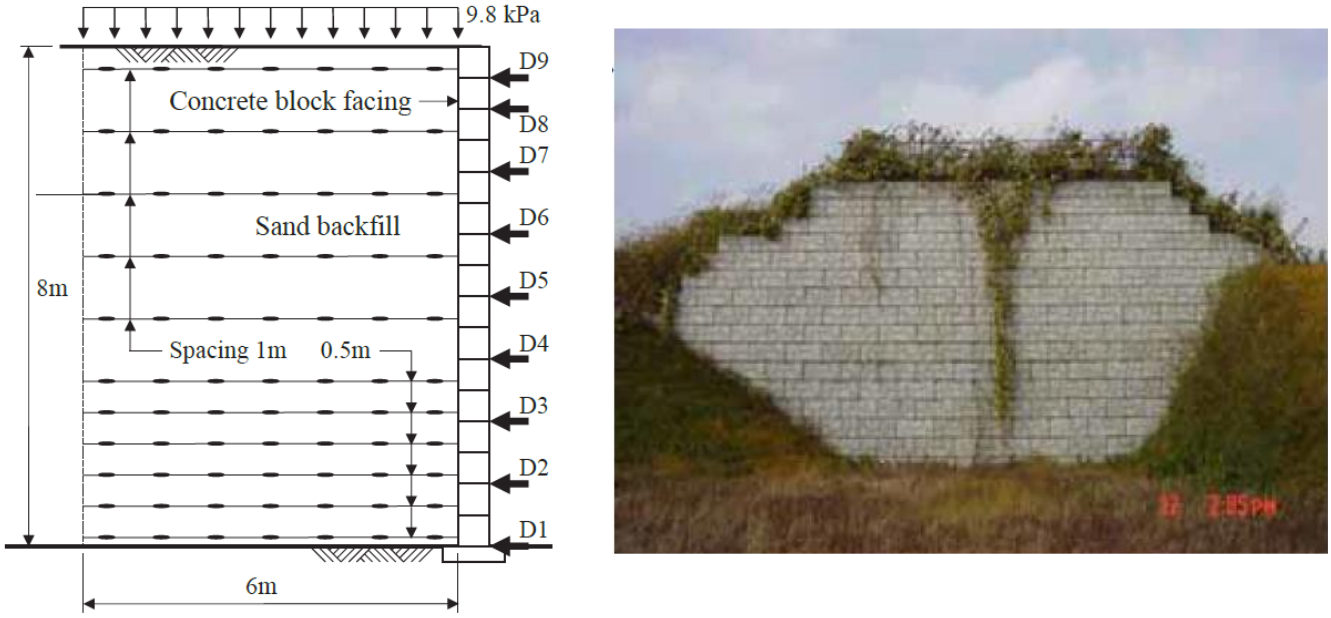

Figure 6. Cross-section (from Dobie and McCombie, 2015) and front view of Type 3 wall constructed in 1995 (from Onodera et Al, 2004)

Table 2. Results of stability calculations for the wall described by Dobie and McCombie (2015)

#	Geogrid Elevation [m]	Tavailable [kN/m]	Tmax [kN/m]	Tmd [kN/m]	Specified minimum Fs-overall static	Actual calculated Fs-overall static
1	0.15	29.5	15.4	N/A	1.000	1.913
2	0.65	29.5	18.2	N/A	1.000	1.618
3	1.15	29.5	17.1	N/A	1.000	1.728
4	1.65	29.5	15.9	N/A	1.000	1.853
5	2.15	29.5	14.8	N/A	1.000	1.998
6	2.65	29.5	20.0	N/A	1.000	1.477
7	3.65	29.5	22.6	N/A	1.000	1.306
8	4.65	29.5	18.0	N/A	1.000	1.642
9	5.65	29.5	13.4	N/A	1.000	2.210
10	6.65	29.5	8.7	N/A	1.000	3.381
11	7.65	29.5	3.8	N/A	1.000	7.799

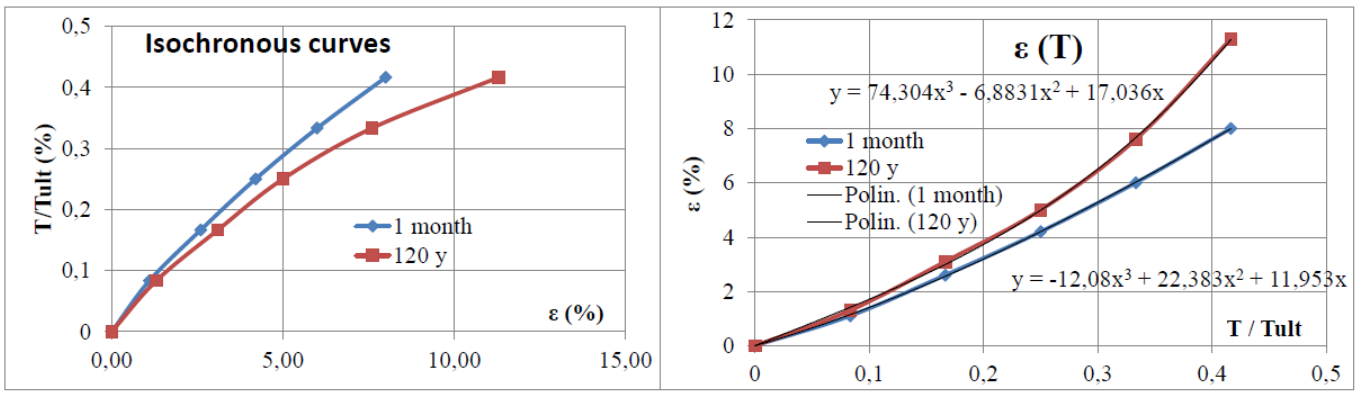

Figure 7. Isochronous curves at 1 months and 120 years (left) and curves $\varepsilon = f(T / T_{ult})$ with interpolation polynomials (right) assumed for Tensar SR55 geogrids

From the published isochronous curves of Tensar SR geogrids, the isochronous curves at 1 months and 120 years and the curves $\varepsilon = f(T / T_{ult})$ at 1 month and at 2 years have been plotted, as shown in Fig. 7, which reports the interpolation polynomials assumed for Tensar SR55 geogrids.
Following the above explained procedure, the horizontal displacements of the wall face at 1 month and at 2 years have been calculated and plotted, as shown in Fig. 8, which also shows the comparison with the displacements reported by Dobie and McCombie (2015): it is easy to see that the maximum lateral movement of the wall, measured as 30 mm approx., is reproduced very well by the Displacement Method. Apart from the different vertical position of the calculation points (coinciding with the positions of the geogrids) and of the survey points, even the pattern of the measured lateral movements, with both convex and concave curvature, is reproduced in a much better way than the prediction with the method of Dobie and McCombie (2015), featuring just single curvature.
Hence this is a first validation that the proposed Displacement Method affords reliable values of lateral movements of a wall.

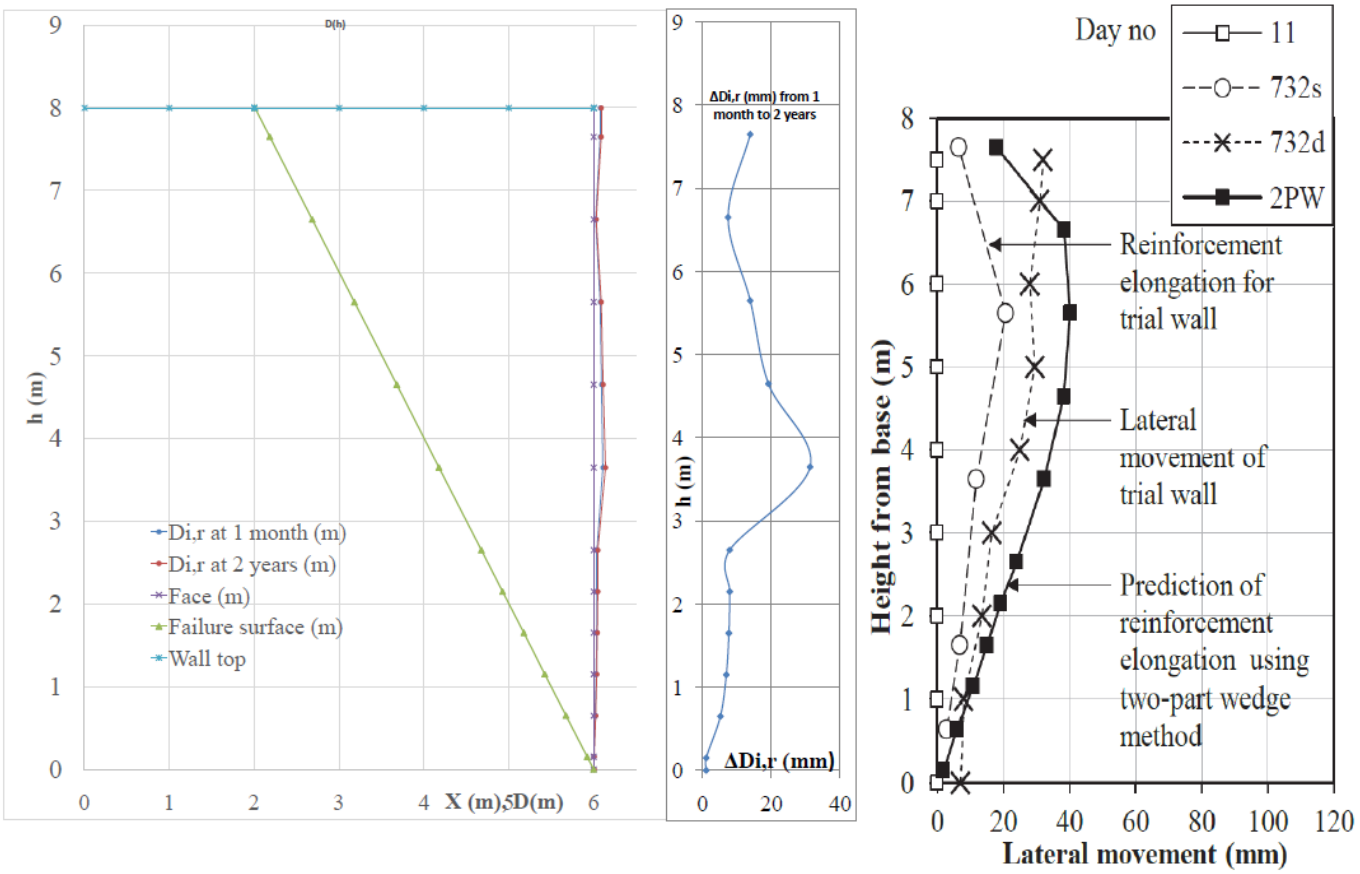

Figure 8. Results of displacement calculations and comparison with displacements reported by Dobie and McCombie (2015)

4.2 *Validation with Gu et Al (2017)*

According to Ozcelik et Al (2014), Tanyu et Al (2016), and Gu et Al (2017), in 2013 a mechanically stabilized earth (MSE) wall, 16 m tall, was constructed in Izmir, Turkey, which is located in a highly seismically active part of the World. For the project, a hybrid reinforced soil system, made up by the combination of both metallic and geosynthetic reinforcement elements, has been adopted for construction of vertical retaining structures and stabilized steep slopes. The metallic elements included gabion basket facings with double twisted wire mesh tails at the bottom extending 3 m into the structure away from the facing. The geosynthetic reinforcement consisted of ParaLink high strength geogrids (PL), which were overlapped with the wire mesh tails creating a frictional connection with gabion baskets. PL are geogrids consisting of a uniaxial array of high strength strips, manufactured from bundles of high molecular weight and high tenacity polyester yarn, coated with a polyethylene sheath. The selected geogrids for the project had a short-term tensile strength of 400 kN/m. The geogrid reinforcement length was 17.5 m (approximately 110 % of wall height) due to highly seismic conditions. The gabion baskets were filled with processed rock ranging between 100 and 200 mm in size. The backfill placed over the double twisted wire mesh and geogrid consisted of a high frictional select fill with $\varphi = 39°$.

Two sections of the Izmir wall were instrumented to evaluate the effect of vertical spacing between the primary reinforcements. One of the sections was constructed with geogrid reinforcements being vertically spaced 1 m apart from each other and the other one with 2 m vertical spacing (geogrid was placed in between every other gabion basket). The latter instrumented section is shown in Fig. 9.

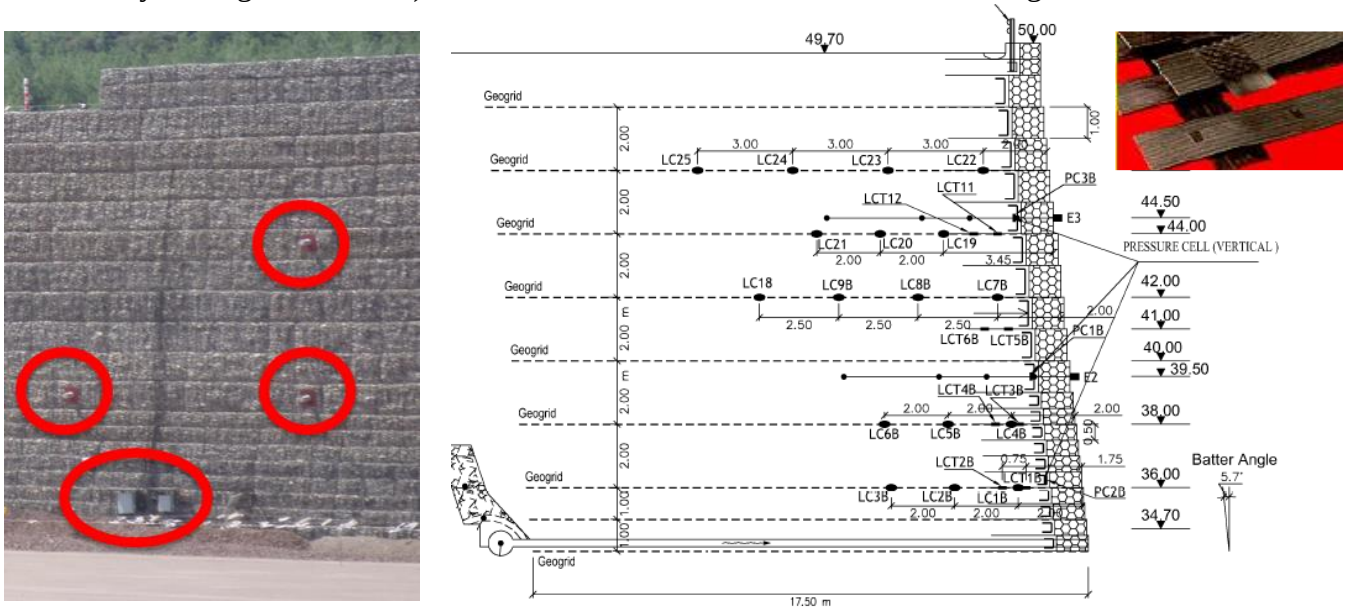

Figure 9. The instrumented sections and the instrumentation layout of the Izmir wall section with primary reinforcement spacing of 2 m; at top right the coated polyester geogrids

Gu et Al (2017) provided the measured and calculated relative horizontal displacements of the wall facing after construction. Two-dimensional finite-difference program FLAC2D 5.0 (Itasca, 2005) was employed to simulate the MSE walls.

For validating the Displacement Method with polyester geogrids and massive facing elements, for the cross-section in Fig. 9 stability analyses were back carried out with MSEW (3.0) software (ADAMA, 2015), affording the maximum tensile strength required for each geogrid layer, as reported in Tab. 3.

From the published isochronous curves of ParaLink geogrids, the isochronous curves at 1 month and 120 years and the curves $\varepsilon = f(T / T_{ult})$ at 1 month and at 120 years have been plotted, as shown in Fig. 10, which reports the interpolation polynomials assumed for ParaLink geogrids.

Following the above explained Displacement Method, the horizontal displacements of the wall face at 1 month and at 120 years have been calculated and plotted, as shown in Fig. 11, which also shows the comparison between the calculated displacements at 1 month and the displacements just after construction reported by Gu et Al (2017): it is easy to see that the maximum lateral movement of the wall, measured as 30 mm approx., is reproduced very well by the Displacement Method.

Hence this is a second validation that the proposed Displacement Method affords reliable values of lateral movements of a wall, in this case with polyester geogrids and massive facing elements.

Table 3. Results of stability calculations for the Izmir wall described by Gu et Al (2017)

#	Geogrid Elevation [m]	Tavailable [kN/m]	Tmax [kN/m]	Tmd [kN/m]	Specified minimum Fs-overall static	Actual calculated Fs-overall static
1	0.00	262.9	19.3	N/A	1.000	13.637
2	0.50	262.9	37.7	N/A	1.000	6.976
3	1.00	262.9	89.1	N/A	1.000	2.950
4	3.00	262.9	127.5	N/A	1.000	2.062
5	5.00	262.9	108.9	N/A	1.000	2.415
6	7.00	262.9	90.3	N/A	1.000	2.913
7	9.00	262.9	71.6	N/A	1.000	3.669
8	11.00	262.9	53.0	N/A	1.000	4.957
9	13.00	262.9	34.4	N/A	1.000	7.636
10	15.00	262.9	17.0	N/A	1.000	15.503

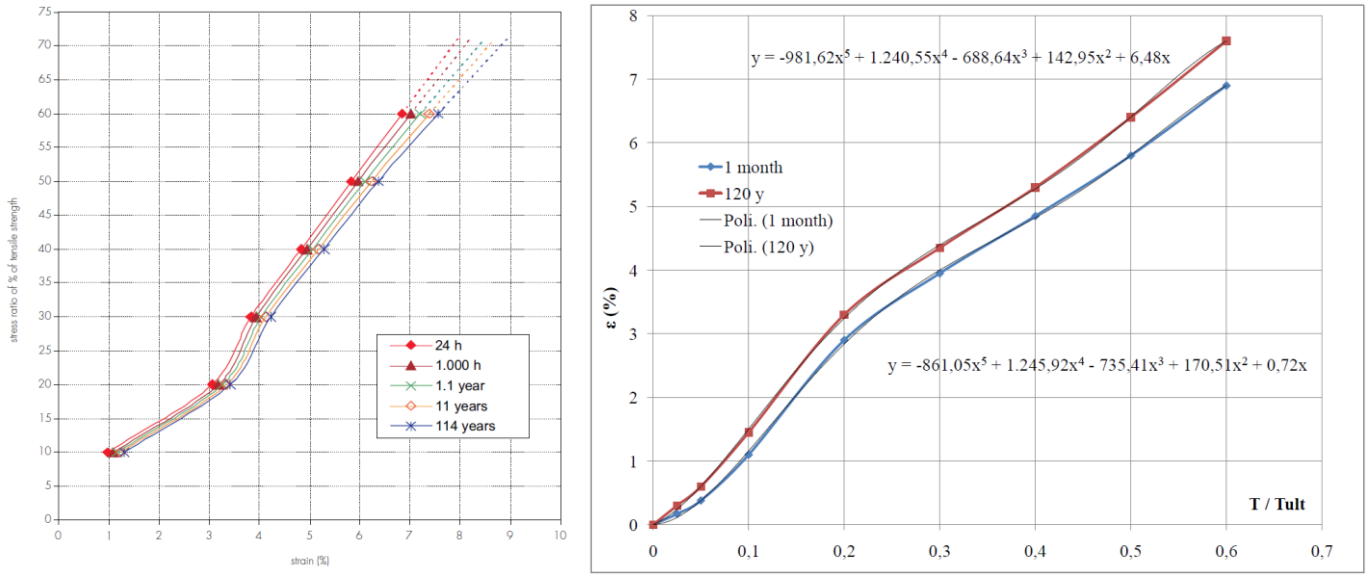

Figure 10. Isochronous curves at 1 months and 120 years (left) and curves $\varepsilon = f(T / T_{ult})$ with interpolation polynomials (right) assumed for ParaLink geogrids

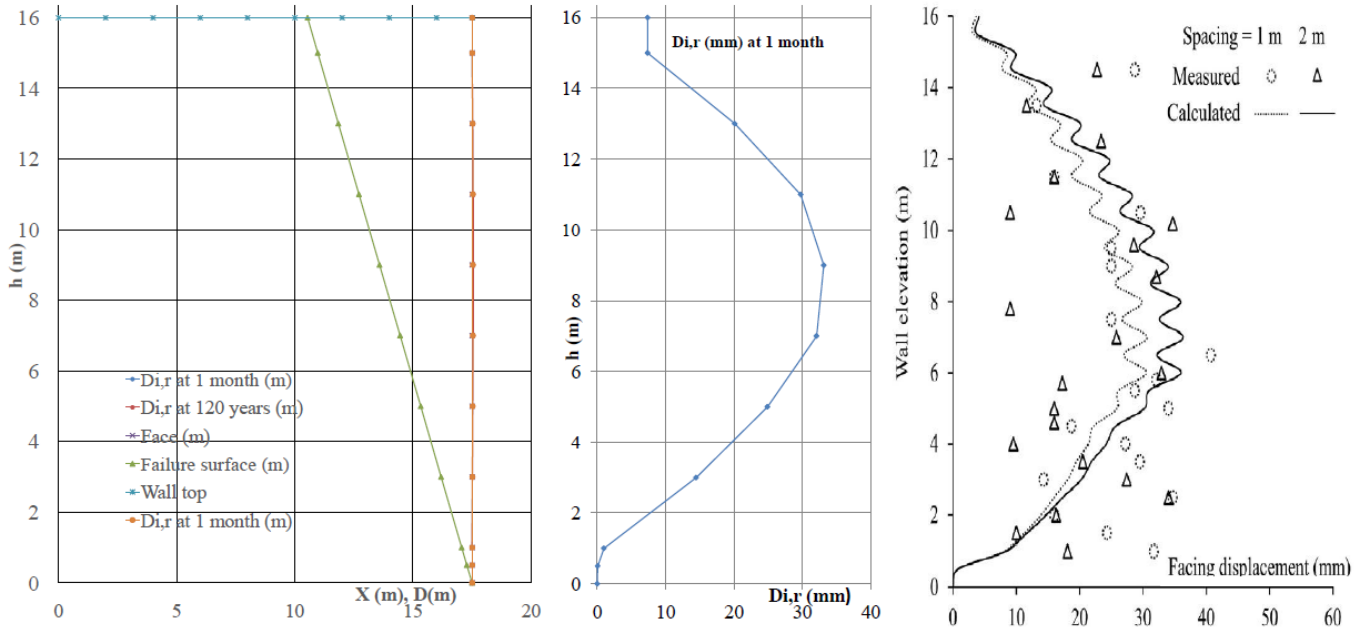

Figure 11. Results of displacement calculations and comparison with displacements just after construction reported by Gu et Al (2017)

5 CONCLUSIONS

A new model is presented for obtaining the horizontal displacements of reinforced soil walls directly from the results of LEM calculations in SLS conditions, which takes into account the position of the maximum tensile strength in each geogrid, the pullout anchorage length, the reduction of tensile strength at face, the restrain at toe, the face batter, the tiers and berms.

Simplified yet realistic hypotheses have been introduced on the distribution of the tensile force along each reinforcement layer, starting from the maximum tensile strength in each layer, which can be easily calculated with a commercial software for stability of reinforced soil walls; the tensile curves and the isochronous curves of each type of reinforcement present in the wall design are used to evaluate the strains associated with the tensile force values, at different elapsed time from construction starting; the integral of the strains along each layer provides the horizontal displacement for that layer; corrections are introduced to reduce the displacements taking into account the stiffness of the facing system and the presence of total or partial restrain at toe.

The Displacement Method has been validated by carrying out calculations for two instrumented walls for which measurements of horizontal displacements are available in literature: comparison with the measured data shows that the proposed method affords realistic value of horizontal displacements.

The proposed Displacement Method can be easily implemented in a spreadsheet, hence it can be a simple and valuable tool for performing the displacement analyses required in SLS conditions.

Finally, the proposed Displacement Method will be eventually expanded to include more situations of practical interest.

REFERENCES

ADAMA (2015). MSEW (Mechanically Stabilized Earth Walls) Version 3.0. ADAMA Engineering, Inc., Clackamas, OR, USA.

BS 8006-1 (2010). Code of practice for strengthened/reinforced soils and other fills. British Standards Institution, London, UK.

Dobie, M.J.D., and McCombie, P.F. (2015). Serviceability limit state check in reinforced soil design. Proc. XVI ECSMGE Geotechnical Engineering for Infrastructure and Development. Edinburgh, UK.

EN 1997-1 (2004). Eurocode 7: Geotechnical design - Part 1: General rules. CEN, Bruxelles, Belgium.

FHWA (2009). Design and Construction of Mechanically Stabilized Earth Walls and Reinforced Soil Slopes – Volume I. National Highway Institute, Federal Highway Administration, U.S. Department of Transportation, Washington, D.C., USA.

Gu, M., Collin, J. G., Han, J., Zhang, Z., Tanyu, B. F., Leshchinsky, D., Ling, H. I., Rimoldi, P. (2017). Numerical analysis of instrumented mechanically stabilized gabion walls with large vertical reinforcement spacing. Geotextiles and Geomembranes (2017).

Itasca Consulting Group (2005). FLAC-fast Lagrangian Analysis of Continua. Version 5.0. Itasca Consulting Group Inc., Minneapolis, MN, USA.

Leshchinsky, D. (2002). "Design software for geosynthetic-reinforced soil structures." Geotechnical Fabrics Report, October/November, 2(8), 44-49.

Nakajima, T. Toriumi, N. Shintani, H. Miyatake, H. & Dobashi, K. (1996). Field performance of a geotextile reinforced soil wall with concrete facing blocks, Proceedings, International Symposium on Earth Reinforcement (IS Kyushu '96) 1, 427–432, Balkema, Rotterdam.

Onodera, S. Fukuda, N. & Nakane, A. (2004). Long-term behavior of geogrid reinforced soils, Proceedings, Sixth International Conference on Geosynthetics 2, 577–580, Atlanta, USA.

Ozcelik, H., Gamberini, D., Pezzano, P., & Rimoldi, P. (2014), "Geogrid and double twist steel mesh reinforced soil walls subjected to high loads in a seismic area", Proceedings of 10th International Conference on Geosynthetics, Berlin, Germany.

Tanyu, B.F., Abbaspour , A., Collin, J.G., Leshchinshy, D., Han, J., Ling, H.I., & Rimoldi, P. (2016). Case study: instrumentation of a hybrid MSE wall system with up to 2 m vertical spacing between reinforcements. In: 3rd Pan American Conference on Geosynthetics, GeoAmericas, Miama, FL, USA.

Tsukada, Y., Ochiai, Y., Miyatake, H. & Tajiri, N. (1998). Field performance test of a geosynthetic-reinforced soil wall with rigid facing, Proceedings, GeoAsia 2004, 225–264, Seoul, Korea.